Original Article

Medial clear space volume on cone beam CT scan offers objective measurement of congruency in supination external rotation ankle fractures in a cadaver model

Mark C. Lawlor, Zachary Zimmer, Melissa A. Kluczynski, John M. Marzo

Department of Orthopaedics, The Jacobs School of Medicine and Biomedical Sciences, The State University of New York, University at Buffalo, Buffalo, NY, USA

Correspondence to: Melissa A. Kluczynski. Department of Orthopaedics, The Jacobs School of Medicine and Biomedical Sciences, The State University of New York, University at Buffalo, Buffalo, NY, USA. Email: mk67@buffalo.edu.

Background: We performed a volume analysis of gravity stress (GS) and simulated weight bearing (WB) CBCT scans of a cadaveric supination external rotation (SER) ankle fracture model.

Methods: An AO supination external rotation 44B3.1 ankle fracture was simulated in 6 human cadavers, each serving as its own control. MCS volume (mm^3) was measured on GS and WB CBCT scans. Paired t-tests were used to compare the MCS volume for control versus experimental conditions for GS and WB conditions, and means ± standard deviation are presented.

Results: MCS on GS CBCT was greater for the experimental (1,540.15±374.8) versus control (984.5±226.5) groups (P=0.004), and MCS on WB CBCT was also greater for the experimental (1,225.57±274.1) versus control (1,059.40±266.6) groups (P=0.05). MCS on GS CBCT was greater for the experimental group compared to both WB CBCT controls (P=0.005) and WB CBCT experimental group (P=0.04). Additionally, MCS on WB CBCT was greater for the experimental group compared to GS CBCT controls (P=0.002), however there was no statistically significant difference in MCS on GS CBCT for controls versus WB CBCT for controls (P=0.08).

Conclusions: MCS volume increased on WB CBCT scans using a cadaveric SER ankle fracture model.

Keywords: Weight bearing (WB); computed tomography (CT); ankle fracture; gravity stress

Submitted Aug 12, 2019. Accepted for publication Dec 03, 2019.
doi: 10.21037/qims.2019.12.08
View this article at: http://dx.doi.org/10.21037/qims.2019.12.08

Introduction

For determining stability of the ankle mortise in a supination external rotation (SER) injury, the gold standard measurement of the medial clear space (MCS) distance has been a manual or gravity stress radiograph (1-4). Weight-bearing (WB) radiographs may be more predictive of stability, and in patients with an anatomically reduced mortise, some authors report successful management nonoperatively with protected WB and functional rehabilitation (2,5-9). WB computed tomography (CT) scans might offer the most accurate view of the ankle mortise under normal stress (10-12).

A substantial amount of malrotation of the distal fibula can be missed on radiographs and contribute to a poor outcome when SER injuries are inadequately reduced (13). Furthermore, MCS distance may not be reliable for determining medial ligamentous damage, and the reliability of MCS measures based on standard radiographs has been debated (14-16). CT scanning provides excellent bone detail and visualization in multiple planes. Marzo *et al.* reported that when SER injuries were evaluated using WBCT, even though the MCS distance was restored, residual findings included posterior malleolar involvement, fibular

© Quantitative Imaging in Medicine and Surgery. All rights reserved.

shortening, fibular rotation, fracture comminution, and asymmetry of the distal tibiofibular joint (8).

Taser *et al.* examined volume changes due to ankle syndesmosis diastasis on three-dimensional renderings of axial CT images, and suggested that calculating the joint space volume may allow a better understanding of the pathoanatomy of tibiofibular diastasis (17). Therefore, we evaluated the MCS volume using similar manual segmentation methodology to investigate the pathoanatomy in a Weber B, SER injury pattern in a cadaveric model.

A previous study reported a technique using a new dedicated extremity cone-beam computed tomography (CBCT) scanner (OnSight 3D Extremity System, Carestream Health, Rochester, NY) to distinguish between stable and unstable injury in an ankle fracture model. While that study used medial clear space distance, our study focuses on changes in MCS volume as a three-dimensional representation of the ankle mortise under gravity stress and weight bearing conditions. We hypothesized that MCS volume would not be different between controls and fractured ankles that showed reduction of the MCS distance on weight bearing CT scan.

Methods

Experimental protocol

Previous research has investigated the use of CT scans to evaluate the condition of the ankle mortise in a cadaveric SER ankle injury fracture model and reported measures of medial clear space *distance*, comparing control to gravity stress and weight bearing conditions (18). For our analysis, control and experimental images from GS and WBCBCT conditions were also used, but medial clear space *volume* was measured. All images were captured with the OnSight 3D Extremity System on specimens mounted in a custom testing rig (*Figure 1A*). First, a GSCBCT scan was obtained by rotating the gantry of the CT scanner to a vertical position, where the testing rig and specimen could be inserted so that the ankle could move freely under the force of gravity (*Figure 1B*). To obtain WB images, a load of 222 N was then applied to each specimen in the rig, and the fixation bolts were screwed tightly to maintain the load. Each loaded specimen underwent CT scanning after rotation of the gantry back to a horizontal position (*Figure 1C*).

After control images were obtained for each of 6 specimens, a fracture model was created in accordance with Park *et al.* In sequence, through a lateral incision the anterior tibiofibular ligament was transected, the fibula osteotomized, and the posterior tibiofibular ligament transected. Through a medial incision, the deep and superficial components of the deltoid ligament were completely incised. Once the fracture model was complete, the same sequence of imaging was performed as described above (19). For every condition, the width of the MCS was measured as the distance between the lateral border of the medial malleolus and the medial border of the talus at the level of the talar dome (20-22). The ankle MCS was measured for all samples using the digital line tool of a Picture Archiving and Communication System.

Determining medial clear space volume

The MCS volume for each ankle was calculated using 3D Slicer Version 4.9.0 (www.slicer.org), an open source software platform with a variety of medical imaging applications (Z.Z.) (23). The program displays CT data from all three planes (coronal, sagittal, and axial) in separate windows and is able to link them in such a way that edits in one plane simultaneously appear in the other two. This connection allows the margins of three-dimensional forms representing the MCS volume to be effectively delineated.

For this study, 3D Slicer's "Segment Editor" tool was used for manual segmentation. Starting in the axial plane, a straight line was drawn from the anterior margin of the medial malleolus to the anterior margin of the talus, marking the anterior boundary of the MCS. Another straight line was then drawn from the posterior margin of the medial malleolus to the posterior margin of the talus, marking the posterior boundary of the MCS. Next, the contours of the lateral aspect of the medial malleolus and medial aspect of the talus were outlined and connected to the anterior and posterior lines to close the shape (*Figure 2A*). This method was repeated for each axial slice from the distal extent of the medial malleolus to the superior extent of the talar dome (*Figure 2B*). Consequently, the number of axial slices used for each ankle varied depending on the height of the MCS. To ensure that no part of what may be considered superior clear space contributed to the model, the coronal plane was examined from the anterior margin of the talus to the posterior margin of the talus. Because Slicer links edits in all three CT planes, any volume superior to the superomedial margin of the talus that was drawn in the axial plane was able to be isolated and deleted in the coronal plane. This was a necessary correcting step because

© Quantitative Imaging in Medicine and Surgery. All rights reserved.

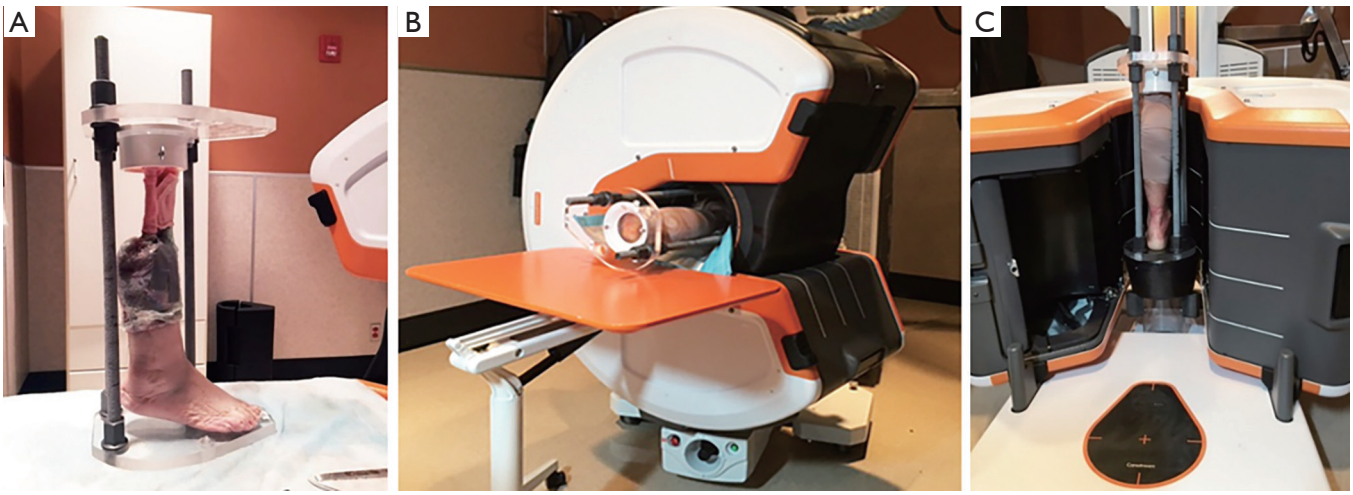

Figure 1 Illustration of experimental testing set up. (A) The testing rig consisted of Plexiglas top and base, each milled to the shape of the cone-beam computed tomography (CBCT) scanner's foot plate. (B) An ankle specimen in the CBCT scanner positioned for a gravity stress scan. (C) An ankle specimen in the CBCT scanner positioned for a weight-bearing scan after 222 N load was simulated.

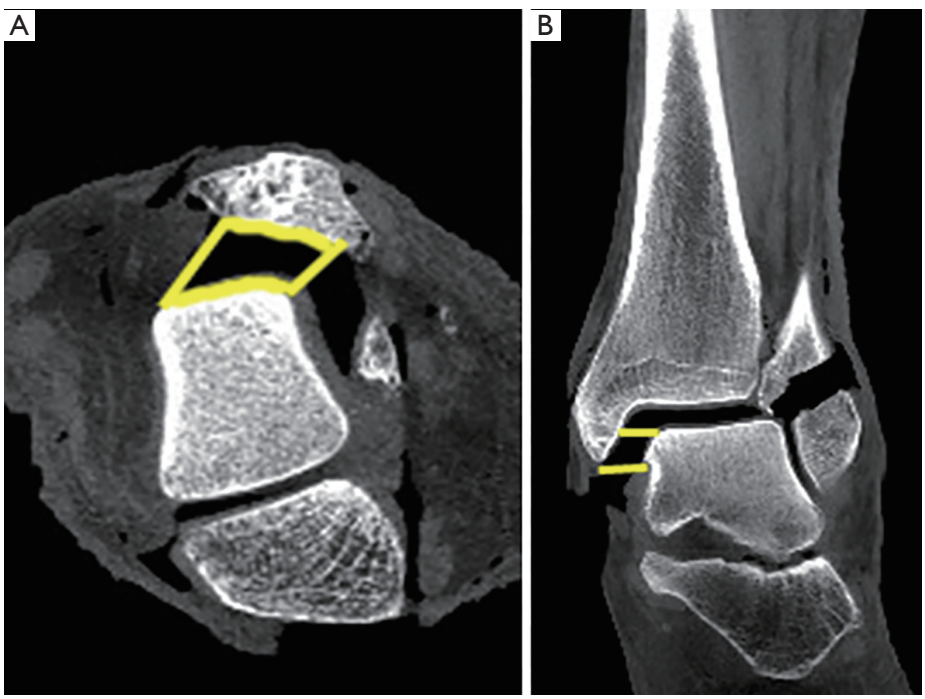

Figure 2 Measurement of MCS volume. (A) An axial view of ankle outlining borders of medial clear space (MCS). (B) Coronal view defines the height of the MCS.

© Quantitative Imaging in Medicine and Surgery. All rights reserved.

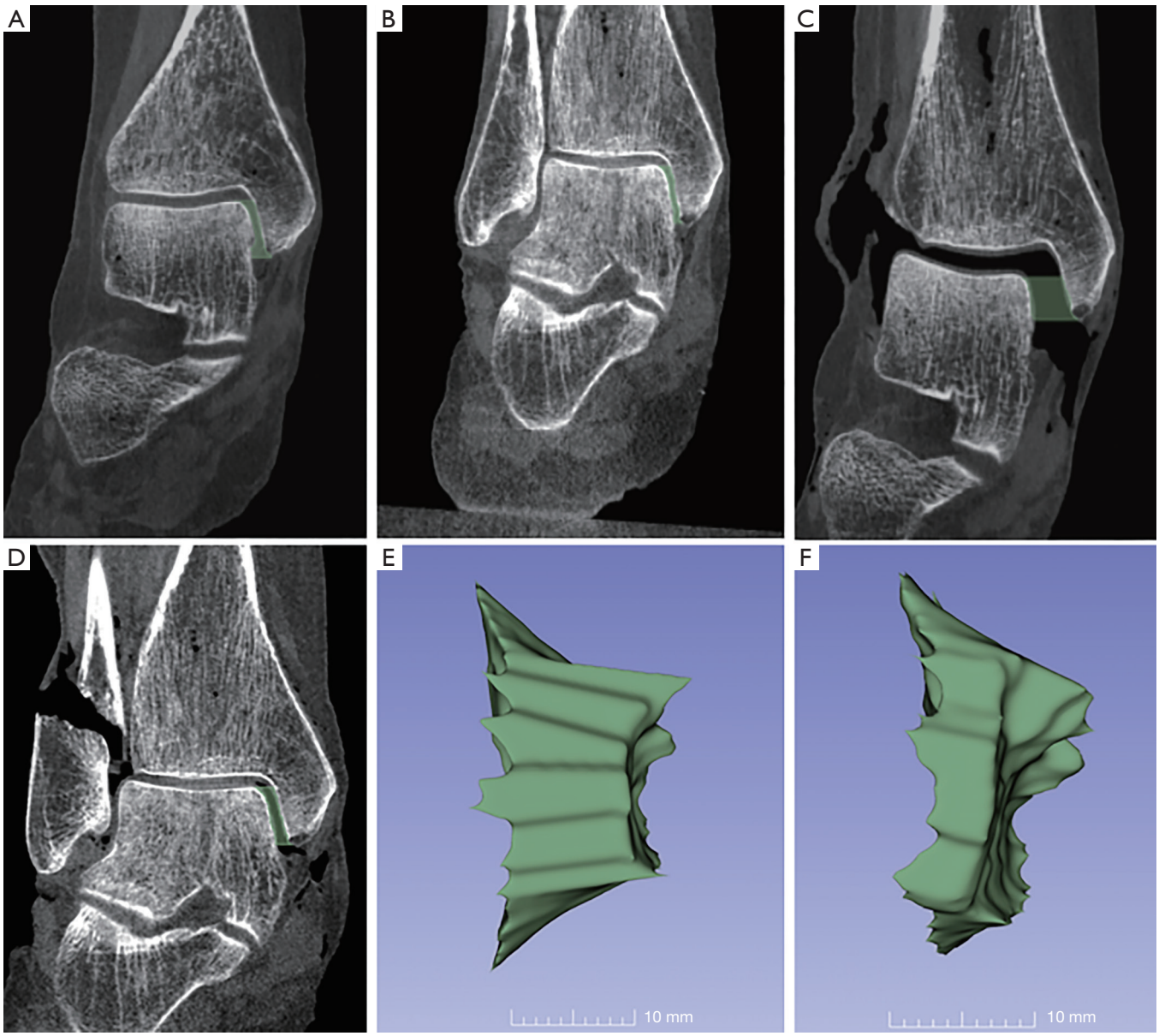

Figure 3 Measurement of MCS volume on gravity-stress and weight bearing images using a software program. (A) A coronal view of ankle mortise outlining borders of medial clear space (MCS) volume in a control specimen in gravity-stress. (B) A coronal view of ankle mortise outlining borders of MCS volume in a control specimen in weight bearing. (C) A coronal view of ankle mortise showing maximum MCS distance in an experimental specimen in gravity-stress condition. (D) A coronal view of ankle mortise showing a reduced MCS distance in an experimental specimen under weight-bearing. (E) Three-dimensional MCS volume rendered from the image seen in Figure 3C (experimental condition under gravity-stress). (F) Three-dimensional MCS volume rendered from the image seen in Figure 3D (experimental condition under weight-bearing stress).

the convexity of the talar dome makes it difficult to discern MCS from superior clear space using the axial plane alone.

The previous steps yield a stack of MCS areas, all in the axial plane, each with 1.0 mm thickness due to the CT slice parameters. The 3D Slicer's "smoothing" tool was utilized to merge the stack of areas into one contiguous figure; the desired three-dimensional model of the MCS, and the software calculates its volume (*Figure 3*). Previous studies

© Quantitative Imaging in Medicine and Surgery. All rights reserved.

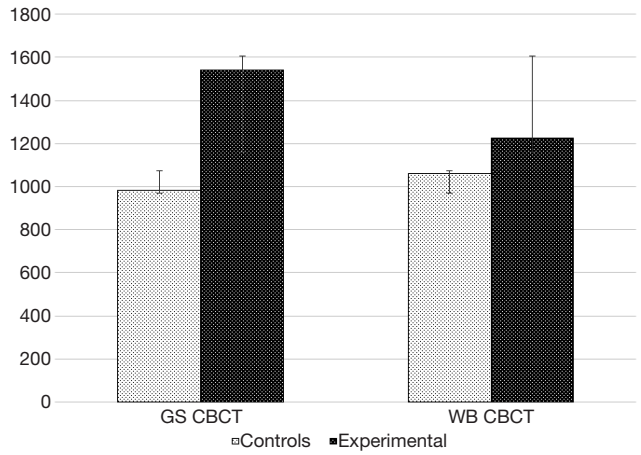

Figure 4 Comparison of volume (mm^3) on gravity-stress (GS) versus weight-bearing (WB) cone beam computed tomography (CBCT) scan.

using similar software have shown good reliability between raters (17,24).

Statistical analysis

Paired *t*-tests were used to compare the MCS volume for control versus experimental conditions for GSCBCT and WBCBCT scans. Also, comparisons of MCS volume for GSCBCT versus WBCBCT scans for control and experimental conditions were made. Each ankle served as its own control prior to creation of the fracture model. Means ± standard deviation are reported, and SAS 9.4 (SAS Institute, Cary, NC) was used for statistical analysis.

Results

For the 6 specimens, mean volume (mm^3) on GSCBCT was greater for the experimental (1,540.15±374.8) versus control (984.5±226.5) groups (P=0.004, *Figure 4*). There was also a difference in mean volume (mm^3) on WBCBCT for the experimental (1,225.57±274.1) versus control (1,059.40±266.6) groups (P=0.05, *Figure 4*). As shown in *Figure 4*, mean volume (mm^3) on GSCBCT was greater for the experimental group compared to both WBCBCT controls (P=0.005) and WBCBCT experimental group (P=0.04). Additionally, mean volume (mm^3) on WBCBCT was greater for the experimental group compared to GSCBCT controls (P=0.002), however there was no statistically significant difference in mean volume on GSCBCT for controls versus WBCBCT for controls (P=0.08).

To illustrate these findings, compared with controls assessed by GSCBCT, the MCS volume was statistically significantly greater for the experimental condition and showed a mean increase in volume of 36%. This was an anticipated result, as the nature of a GS image induces a destabilizing force. *Figure 3A,B* show the control condition under gravity stress and weight bearing, respectively. *Figure 3C,E* of the experimental condition depict a dramatic increase in MCS distance and in the three-dimensional volume rendering. *Figures 3D,F* depicts the MCS of the experimental condition decreased under WB as well as in the three-dimensional volume rendering. In the single ankle, despite a normal MCS distance, the MCS volume of the WB experimental (*Figure 5*) is greater than that of the WB control ankle (*Figure 5*). This observation is most clearly demonstrated by volume data calculated from the specific specimen in *Figure 5* which revealed a 39% increase in MCS volume from WBCBCT (966 mm^3 for WBCBCT control *vs.* 1,344 mm^3 for WBCBCT experimental group).

Discussion

The most significant finding of this study is that the volume of the MCS remained elevated despite the seemingly stabilizing effect of simulated weight bearing. When analyzing the change in volume of this group of ankles (where MCS distance <4 mm), the volume increased by a mean of 16%. This result was an unexpected finding and did not support our hypothesis that the effect of WB and apparent anatomical coronal plane reduction of the mortise would not show a significant change in MCS volume.

A prior study using this experimental design to measure MCS distance revealed two subsets of ankles with WB on a Weber B fracture model; a "stable" group in which the talus reduced anatomically in the mortise and an "unstable" group where the MCS distance was increased (18). These results suggest that measuring MCS distance on a WBCBCT scan may be able to distinguish between potentially stable and unstable fractures and, by extension, determine which ankles may be considered for operative intervention.

Marzo *et al.* reported that when SER injuries were evaluated using WBCT, even though the MCS distance was restored, residual findings included fibular shortening, fibular rotation, fracture comminution, asymmetry of the distal tibiofibular joint, and posterior malleolar involvement (8). Our volumetric analysis suggests that most of the displacement in Weber B fractures must be in planes

© Quantitative Imaging in Medicine and Surgery. All rights reserved.

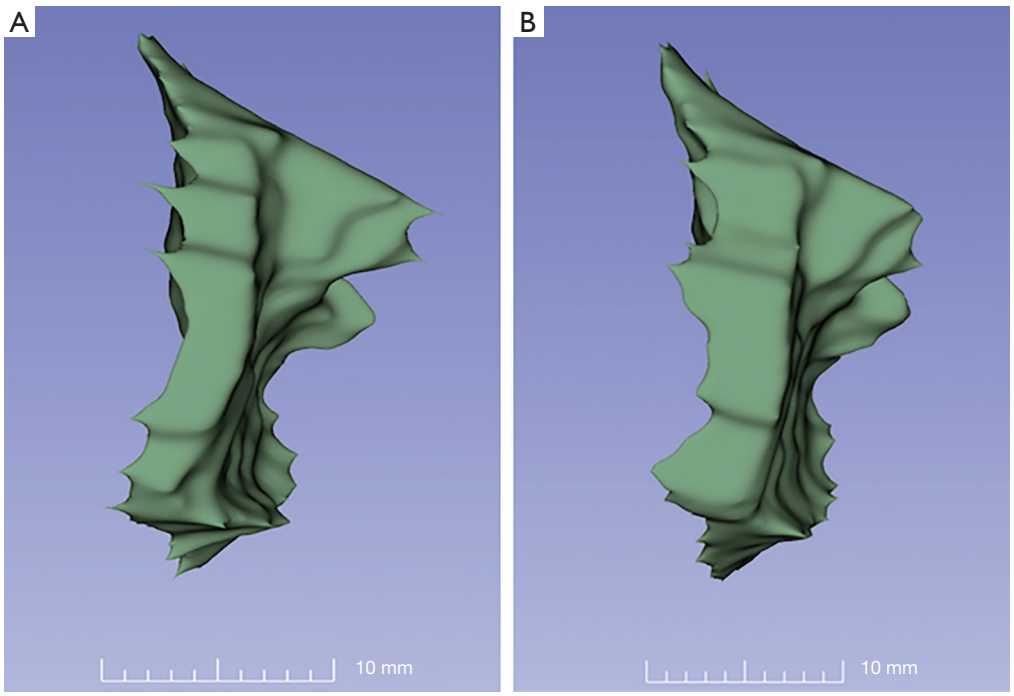

Figure 5 Three-dimensional images of MCS volume. (A) Three-dimensional medial clear space (MCS) volume rendered from the image seen in *Figure 3B* (control specimen under weight-bearing). MCS volume is 966 mm^3. (B) Three-dimensional MCS volume rendered from the image seen in 3D (experimental specimen under weight-bearing). MCS volume is 1,344 mm^3.

other than the coronal plane, and that relying solely on measurement of MCS distance on a standard radiography or CT does not capture total residual displacement. Lawlor *et al.* showed a MCS distance increase of 422% on GS radiograph and 360% on GSCT in the same ankle fracture model (18). Displacement was corrected with simulated WB in a subset of specimens. Others have proposed ways to measure fibular rotation on axial CT slices as a measure of residual displacement, but have not been universally adopted (25-28). To our knowledge, this is the first study of its kind to analyze medial clear space volume with the goal of allowing a more accurate analysis of the injury pattern across three planes.

MCS distance measurement can be a quick, easy, and readily available patient management tool, but its limitation must be recognized as a uniplanar image of a complex joint. Bone overlap and variability in ankle position and radiographic technique are some of many factors that can make interpretation of radiographs difficult in SER ankle fracture evaluations (14-16). CT scans are better than radiographs for visualization of bone detail, and by review of 2D multiplanar images as well as 3D reconstructions, they can be helpful for assessing the complicated anatomy of fractures or dislocations in the musculoskeletal system (13,14,29,30).

Dawe *et al.* proposed the idea of a "stability reserve", where ankles with partial deep deltoid ligament tears will have a widened MCS on GS views due to the destabilizing effect of gravity but will reduce on WB, whereas ankles with complete deep deltoid ligament disruption will not reduce on WB (31). A previous experimental model consisted of complete transection of deep and superficial deltoid as well as anterior inferior tibiofibular ligament and posterior inferior tibiofibular ligament and 6 out of 10 ankles still reduced under WB based on MCS distance measurement, suggesting a stabilizing force for even the unstable ankle (18). Sanders *et al.* studied 81 patients with nondisplaced, unstable isolated lateral malleolus fractures with MCS >5 mm as determined by external rotation manual stress test (32). Nonsurgical management of these patients had a 20% incidence of persistent mal-aligned mortise defined by MCS >5 mm as well as increased risk of fracture displacement (32). Similarly, Willett *et al.* found that patients with non-operative treatment of nondisplaced, unstable ankles had a malunion rate of 15% compared to that of 3% in the operative group (33).

© Quantitative Imaging in Medicine and Surgery. All rights reserved.

Kwon *et al.* estimated that 10–20% of patients with stress-positive ankles develop a mal-aligned mortise if treated non-operatively and there have been few signs detected on initial radiographs that reliably predict this complication (34). According to Kwon *et al.*, the clinical significance of an ankle mortise that appears anatomic when weight is applied, but is non-anatomic in a non-WB position (mortise, GS) remains unclear (35). The data from the current study suggests that a mortise that is apparently anatomically correct on WB may still have a significant increase in MCS volume. We do not know if a 16% increase in MCS volume is a clinically significant difference or has a detrimental biomechanical effect like has been shown from MCS distance. We suggest that future investigations focus on MCS volume and its potential role in clinical outcomes, and changing ankle biomechanics with respect to the development of post-traumatic arthritis following SER ankle fracture. Previous studies have shown 50–55% and 70–77% decreases in tibiotalar contact area for 2 and 4 mm of lateral fibular displacement, respectively. They also yielded a 39% and 70% decrease in contact area for 2 and 4 mm of posterior/superior displacement, respectively (21,36). It has been recognized that even slight changes in MCS distance can have considerable consequences for tibiotalar articulation. No studies have correlated a MCS volume increase with change in tibiotalar contact area, an area of interest for future study.

Potential limitations of this study are a small sample size and that testing was performed on cadaveric ankles under a simulated WB load. We were limited in stacking weights on our testing rig, so our applied load of 222 N is less than in other biomechanical studies of the ankle, and less than physiological for either bipedal or unipedal weight bearing. We used fresh frozen cadaveric specimens for this study and recognize that temperature and time of exposure before testing were variable. These factors may have altered the mechanical properties of bone, ligament, and tendon. It is also possible that because of the viscoelastic properties of the articular cartilage and bone, the load applied for simulation of WB may have attenuated over the time that specimens were imaged. Our model was that of an end stage SER ankle injury, with complete deficiency of the deltoid ligament, and we do not know if our conclusions apply to lesser degrees of injury where the status of the deltoid ligament is in question. We do not know if patients with damage to the bone and soft tissue of the ankle, similar to those created in our model, would be able to withstand WB for the duration of a cone beam CT scan, especially if the talus displaces in the ankle mortise while standing. Delineating the boundaries of a three-dimensional MCS is also somewhat arbitrary, and not detailed in the literature, but a previously reported method for volume calculation using 3D modeling showed good reliability between raters (17,24). More efficient methods are needed for the calculation of MCS volume to be practical, and it is hopeful that a fast manual segmentation or fully automatic technique will be developed in the near future to make this measurement more practical.

In conclusion, this study found that the volume of the MCS in an ankle fracture model remained elevated despite the stabilizing effect of simulated WB.

Acknowledgments

None.

Footnote

Conflicts of Interest: This study was funded by Carestream Health, Inc.

References

1. Gill JB, Risko T, Raducan V, Grimes JS, Schutt RC Jr. Comparison of manual and gravity stress radiographs for the evaluation of supination-external rotation fibular fractures. J Bone Joint Surg Am 2007;89:994-9.
2. Weber M, Burmeister H, Flueckiger G, Krause FG. The use of weightbearing radiographs to assess the stability of supination-external rotation fractures of the ankle. Arch Orthop Trauma Surg 2010;130:693-8.
3. Michelson JD, Varner KE, Checcone M. Diagnosing deltoid injury in ankle fractures: the gravity stress view. Clin Orthop Relat Res 2001;(387):178-82.
4. Schock HJ, Pinzur M, Manion L, Stover M. The use of gravity or manual-stress radiographs in the assessment of supination-external rotation fractures of the ankle. J Bone Joint Surg Br 2007;89:1055-9.
5. Hastie GR, Akhtar S, Butt U, Baumann A, Barrie JL. Weightbearing Radiographs Facilitate Functional Treatment of Ankle Fractures of Uncertain Stability. J Foot Ankle Surg 2015;54:1042-6.
6. Hoshino CM, Nomoto EK, Norheim EP, Harris TG. Correlation of weightbearing radiographs and stability of stress positive ankle fractures. Foot Ankle Int 2012;33:92-8.

© Quantitative Imaging in Medicine and Surgery. All rights reserved.

7. Holmes JR, Acker WB, 2nd, Murphy JM, McKinney A, Kadakia AR, Irwin TA. A Novel Algorithm for Isolated Weber B Ankle Fractures: A Retrospective Review of 51 Nonsurgically Treated Patients. J Am Acad Orthop Surg 2016;24:645-52.
8. Marzo JM, Kluczynski MA, Clyde C, Anders MJ, Mutty CE, Ritter CA. Weight bearing cone beam CT scan versus gravity stress radiography for analysis of supination external rotation injuries of the ankle. Quant Imaging Med Surg 2017;7:678-84.
9. Seidel A, Krause F, Weber M. Weightbearing vs Gravity Stress Radiographs for Stability Evaluation of Supination-External Rotation Fractures of the Ankle. Foot Ankle Int 2017;38:736-44.
10. Hirschmann A, Pfirrmann CW, Klammer G, Espinosa N, Buck FM. Upright cone CT of the hindfoot: comparison of the non-weight-bearing with the upright weight-bearing position. Eur Radiol 2014;24:553-8.
11. Carrino JA, Al Muhit A, Zbijewski W, Thawait GK, Stayman JW, Packard N, Senn R, Yang D, Foos DH, Yorkston J, Siewerdsen JH. Dedicated cone-beam CT system for extremity imaging. Radiology 2014;270:816-24.
12. Tuominen EK, Kankare J, Koskinen SK, Mattila KT. Weight-bearing CT imaging of the lower extremity. AJR Am J Roentgenol 2013;200:146-8.
13. Sagi HC, Shah AR, Sanders RW. The functional consequence of syndesmotic joint malreduction at a minimum 2-year follow-up. J Orthop Trauma 2012;26:439-43.
14. Gardner MJ, Demetrakopoulos D, Briggs SM, Helfet DL, Lorich DG. Malreduction of the tibiofibular syndesmosis in ankle fractures. Foot Ankle Int 2006;27:788-92.
15. Dikos GD, Heisler J, Choplin RH, Weber TG. Normal tibiofibular relationships at the syndesmosis on axial CT imaging. J Orthop Trauma 2012;26:433-8.
16. Nault ML, Hebert-Davies J, Laflamme GY, Leduc S. CT scan assessment of the syndesmosis: a new reproducible method. J Orthop Trauma 2013;27:638-41.
17. Taser F, Shafiq Q, Ebraheim NA. Three-dimensional volume rendering of tibiofibular joint space and quantitative analysis of change in volume due to tibiofibular syndesmosis diastases. Skeletal Radiol 2006;35:935-41.
18. Lawlor MC, Kluczynski MA, Marzo JM. Weight-Bearing Cone-Beam CT Scan Assessment of Stability of Supination External Rotation Ankle Fractures in a Cadaver Model. Foot Ankle Int 2018;39:850-7.
19. Park SS, Kubiak EN, Egol KA, Kummer F, Koval KJ. Stress radiographs after ankle fracture: the effect of ankle position and deltoid ligament status on medial clear space measurements. J Orthop Trauma 2006;20:11-8.
20. Egol KA, Amirtharajah M, Tejwani NC, Capla EL, Koval KJ. Ankle stress test for predicting the need for surgical fixation of isolated fibular fractures. J Bone Joint Surg Am 2004;86:2393-8.
21. Harris J, Fallat L. Effects of isolated Weber B fibular fractures on the tibiotalar contact area. J Foot Ankle Surg 2004;43:3-9.
22. Joy G, Patzakis MJ, Harvey JP Jr. Precise evaluation of the reduction of severe ankle fractures. J Bone Joint Surg Am 1974;56:979-93.
23. Fedorov A, Beichel R, Kalpathy-Cramer J, Finet J, Fillion-Robin JC, Pujol S, Bauer C, Jennings D, Fennessy F, Sonka M, Buatti J, Aylward S, Miller JV, Pieper S, Kikinis R. 3D Slicer as an image computing platform for the Quantitative Imaging Network. Magn Reson Imaging 2012;30:1323-41.
24. Velazquez ER, Parmar C, Jermoumi M, Mak RH, van Baardwijk A, Fennessy FM, Lewis JH, De Ruysscher D, Kikinis R, Lambin P, Aerts HJ. Volumetric CT-based segmentation of NSCLC using 3D-Slicer. Sci Rep 2013;3:3529.
25. Gifford PB, Lutz M. The tibiofibular line: an anatomical feature to diagnose syndesmosis malposition. Foot Ankle Int 2014;35:1181-6.
26. Zwipp H. Chirurgie des Fusses. Wien: Springer-Verlag; 1994.
27. Knops SP, Kohn MA, Hansen EN, Matityahu A, Marmor M. Rotational malreduction of the syndesmosis: reliability and accuracy of computed tomography measurement methods. Foot Ankle Int 2013;34:1403-10.
28. Lepojärvi S, Niinimaki J, Pakarinen H, Leskela HV. Rotational Dynamics of the Normal Distal Tibiofibular Joint With Weight-Bearing Computed Tomography. Foot Ankle Int 2016;37:627-35.
29. Ebraheim NA, Lu J, Yang H, Mekhail AO, Yeasting RA. Radiographic and CT evaluation of tibiofibular syndesmotic diastasis: a cadaver study. Foot Ankle Int 1997;18:693-8.
30. Ebraheim NA, Elgafy H, Padanilam T. Syndesmotic disruption in low fibular fractures associated with deltoid ligament injury. Clin Orthop Relat Res 2003;(409):260-7.
31. Dawe EJ, Shafafy R, Quayle J, Gougoulias N, Wee A, Sakellariou A. The effect of different methods of stability assessment on fixation rate and complications in supination external rotation (SER) 2/4 ankle fractures. Foot Ankle

© Quantitative Imaging in Medicine and Surgery. All rights reserved.

Surg 2015;21:86-90.
32. Sanders DW, Tieszer C, Corbett B, Canadian Orthopedic Trauma S. Operative versus nonoperative treatment of unstable lateral malleolar fractures: a randomized multicenter trial. J Orthop Trauma 2012;26:129-34.
33. Willett K, Keene DJ, Mistry D, Nam J, Tutton E, Handley R, Morgan L, Roberts E, Briggs A, Lall R, Chesser TJ, Pallister I, Lamb SE; Ankle Injury Management (AIM) Trial Collaborators. Close Contact Casting vs Surgery for Initial Treatment of Unstable Ankle Fractures in Older Adults: A Randomized Clinical Trial. JAMA 2016;316:1455-63.
34. Kwon JY, Cronin P, Velasco B, Chiodo C. Evaluation and Significance of Mortise Instability in Supination External Rotation Fibula Fractures: A Review Article. Foot Ankle Int 2018;39:865-73.
35. Kwon JY. Letter Regarding: Weightbearing vs Gravity Stress Radiographs for Stability Evaluation of Supination-External Rotation Fractures of the Ankle. Foot Ankle Int 2017;38:1400-1.
36. Lloyd J, Elsayed S, Hariharan K, Tanaka H. Revisiting the concept of talar shift in ankle fractures. Foot Ankle Int 2006;27:793-6.

Cite this article as: Lawlor MC, Zimmer Z, Kluczynski MA, Marzo JM. Medial clear space volume on cone beam CT scan offers objective measurement of congruency in supination external rotation ankle fractures in a cadaver model. Quant Imaging Med Surg 2020;10(2):380-388. doi: 10.21037/qims.2019.12.08

© Quantitative Imaging in Medicine and Surgery. All rights reserved.